

Thermal Denaturation of Fluctuating DNA Driven by Bending Entropy

J. Palmeri, M. Manghi and N. Destainville

Laboratoire de Physique Théorique, Université de Toulouse, CNRS, 31062 Toulouse, France

(Dated: February 4, 2018)

A statistical model of homopolymer DNA, coupling internal base pair states (unbroken or broken) and external thermal chain fluctuations, is exactly solved using transfer kernel techniques. The dependence on temperature and DNA length of the fraction of denaturation bubbles and their correlation length is deduced. The *thermal denaturation transition* emerges naturally when the chain fluctuations are integrated out and is driven by the difference in bending (entropy dominated) free energy between broken and unbroken segments. Conformational properties of DNA, such as persistence length and mean-square-radius, are also explicitly calculated, leading, e.g., to a coherent explanation for the experimentally observed *thermal viscosity transition*.

PACS numbers: 87.10.+e, 87.15.Ya, 82.39.Pj

Double-stranded DNA (dsDNA) is made up of two intertwined interacting semi-flexible single-strand DNA (ssDNA) chains. Over fifty years ago it was recognized that the intracellular unwinding of DNA at physiological temperature has as counterpart the thermally induced denaturation above physiological temperature of purified DNA solutions where dsDNA completely separates into two ssDNA. Despite the differences between the two mechanisms, this observation has led to an intensive study of thermal denaturation [1, 2]. The stability of dsDNA at physiological temperature is due to the self-assembly of neighboring base pairs within a same strand *via* base-stacking interactions and of both strands *via* hydrogen bonds between complementary bases. The bonding energy is, however, on the order of $k_B T$ (thermal energy) [3] and thermal fluctuations can lead, even at physiological temperature, to local and transitory unzipping of dsDNA [1]. The cooperative opening of consecutive base pairs leads to denaturation bubbles and the melting temperature, T_m , above which bubbles proliferate, depends on sequence, chain length, and ionic strength. Experiments show, for example, that there exist a bubble initiation barrier of $\sim 10k_B T$ and free energy cost of $\sim 0.1k_B T$ for breaking an additional base pair in an existing A-T bubble [4]. A detailed understanding of equilibrium [1] and dynamical [5] properties of DNA in solution is still being sought and a consensus concerning the physical mechanism behind the denaturation transition has not yet been reached.

A variety of mesoscopic models have been proposed to account for the thermodynamical properties of denaturation bubbles in DNA. They range from i) simple effective Ising-like two-state models [1] to more detailed ones such as ii) loop entropy models (with or without chain self-avoidance) [1, 2, 6, 7], and iii) non-linear phonon models, where the shape of the interaction potential between base pairs is more precisely taken into account [8, 9]. To get a transition in models i) and ii), an effective temperature dependent base-pair chemical potential must be inserted by hand. For finite chains, type (ii) models simply refine

the sharpness of the transition [1], but do not attempt to provide a deeper explanation of the physical mechanism – our aim here. For type (iii) models it has been shown that there can be a denaturation transition analogous to interface unbinding, due to a gain in translational entropy. If, however, physically reasonable values for the model parameters are used [8, 9, 10], T_m appears to be much too high and the transition width much too large.

It has been shown experimentally that dsDNA is two orders of magnitude stiffer than ssDNA at normal salt concentration. We show in this Letter that taking into account this difference in *bending rigidity* provides a novel physical explanation for the denaturation mechanism and leads to realistic values for transition temperatures and widths. Despite important recent advances in understanding the crucial role played by DNA *bending rigidity* in explaining force-extension [11, 12] and cyclization [13] experiments, its importance has not yet been clearly elucidated in the context of denaturation. We show, *via* a well-defined coupled Ising-Heisenberg statistical model, that an entropy driven denaturation transition emerges by integrating out chain fluctuations, due to the entropic lowering of the energetic barrier for bubble nucleation. This minimal model neglects all other (residual) interactions between bases arising from, e.g., electrostatics [14], self-avoidance [6], and helical twist [15].

We begin by considering a worm like chain (WLC) Hamiltonian $H[\mathbf{r}_1, \mathbf{r}_2]$ for two interacting ssDNA homopolymers of length L :

$$H = \frac{1}{2} \sum_{i=1}^2 \int_0^L ds \left[\frac{3}{2} \kappa_b(\boldsymbol{\rho}(s)) \ddot{\mathbf{r}}_i^2(s) + \frac{3}{2} \kappa_s(\boldsymbol{\rho}(s)) \dot{\mathbf{r}}_i^2(s) \right] + \int_0^L ds V(\boldsymbol{\rho}(s)), \quad (1)$$

where s is the curvilinear index, $\mathbf{r}_i(s)$ is the position of chain i at base position s , and $\boldsymbol{\rho}(s) \equiv \mathbf{r}_1(s) - \mathbf{r}_2(s)$ is the relative (internal) coordinate ($\beta = 1/k_B T$ and $\dot{\mathbf{r}}(s) = \frac{\partial \mathbf{r}}{\partial s}$). The coefficient κ_b is a *bending* elastic modulus that is proportional to the short distance cut-off $\ell_0 \approx 0.34$ nm

(the monomer length) and $\kappa_s(\boldsymbol{\rho}) = 1/[\beta^2 \kappa_b(\boldsymbol{\rho})]$. In order to account for the enhanced stiffness of dsDNA, κ_b must depend on $\boldsymbol{\rho}(s)$, e.g., $\kappa_b(\boldsymbol{\rho}) = \kappa_b^{ss} + \Delta\kappa_b e^{-(\rho - \rho_0)/\lambda}$, where $\Delta\kappa_b \equiv \kappa_b^{ds}/2 - \kappa_b^{ss} > 0$ and $\lambda \sim 1\text{\AA}$ is the range [10]. The persistence length of ssDNA is $\ell_p^{ss} = \beta\kappa_b^{ss} \approx 1\text{ nm}$ and that of dsDNA is $\ell_p^{ds} = \beta\kappa_b^{ds} \approx 50\text{ nm}$ (at 300 K and physiological ionic strength). The potential $V(\rho)$ accounts for both the effective short range hydrogen bonding interaction between complementary bases at the same s and part of the stacking interaction between neighboring bases; a convenient form is the Morse potential: $V(\rho) = (D/\ell_0)v((\rho - \rho_0)/\lambda)$ where $v(x) = e^{-2x} - 2e^{-x}$, leading to a well depth of D/ℓ_0 at ρ_0 [8].

At high temperature, $\rho(s) - \rho_0 \gg \lambda$, and therefore the system decouples into two semi-flexible non-interacting ssDNA chains. After introducing the center-of-mass (external) coordinate, $\mathbf{X}(s) \equiv [\mathbf{r}_1(s) + \mathbf{r}_2(s)]/2$, the partition function can be rewritten as a sum over center-of-mass and relative configurations: $\mathcal{Q} = \int \mathcal{D}\boldsymbol{\rho} \mathcal{D}\mathbf{X} \exp\{-\beta(H_{\text{ext}}[\mathbf{X}, \boldsymbol{\rho}] + H_{\text{int}}[\boldsymbol{\rho}])\}$, where [16]

$$H_{\text{int}} = \frac{3}{8} \int_0^L ds \left[\kappa_b(\boldsymbol{\rho}) \ddot{\boldsymbol{\rho}}^2 + \kappa_s(\boldsymbol{\rho}) \dot{\boldsymbol{\rho}}^2 + V(\boldsymbol{\rho}) \right] \quad (2)$$

$$H_{\text{ext}} = \frac{3}{2} \int_0^L ds \left[\kappa_b(\boldsymbol{\rho}) \ddot{\mathbf{X}}^2 + \kappa_s(\boldsymbol{\rho}) \dot{\mathbf{X}}^2 \right]. \quad (3)$$

We integrate over \mathbf{X} to obtain an effective model for $\boldsymbol{\rho}$, $\mathcal{Q} = \int \mathcal{D}\boldsymbol{\rho} \exp\{-\beta H_{\text{eff}}[\boldsymbol{\rho}]\}$, where $H_{\text{eff}}[\boldsymbol{\rho}] = H_{\text{int}}[\boldsymbol{\rho}] + \mathcal{F}_{\text{ext}}[\boldsymbol{\rho}]$ with $\mathcal{F}_{\text{ext}}[\boldsymbol{\rho}] = -k_B T \ln \left[\int \mathcal{D}\mathbf{X} \exp\{-\beta H_{\text{ext}}[\mathbf{X}, \boldsymbol{\rho}]\} \right]$. The external free energy $\mathcal{F}_{\text{ext}}[\boldsymbol{\rho}]$ at frozen $\boldsymbol{\rho}$ can be evaluated by introducing the local center-of-mass tangent vectors $\mathbf{t} = \dot{\mathbf{X}}$ and then changing variables to $\tilde{\mathbf{t}} = \mathbf{t}/\sqrt{\kappa_b(\boldsymbol{\rho})}$. There are two contributions to \mathcal{F}_{ext} : one will renormalize the second term in H_{int} and the other will renormalize the potential to V_R . The latter mainly gives rise to a purely entropic barrier favoring bubbles,

$$V_R(\boldsymbol{\rho}) = V(\boldsymbol{\rho}) + \frac{3}{2} \frac{k_B T}{\ell_0} \ln \left[\frac{\kappa_b(\boldsymbol{\rho})}{\kappa_b^{ss}} \right], \quad (4)$$

which lowers the well depth from D to $D_R \approx D - (3/2)k_B T \ln [\kappa_b^{ds}/(2\kappa_b^{ss})]$. The entropic bending contribution can be extremely important when D is in the commonly accepted range of $1 < D/k_B T < 5$ at $T = 350\text{ K}$ and $\kappa_b^{ds}/(2\kappa_b^{ss}) \simeq 25$. Scaling arguments then show that the melting temperature gets reduced by a factor ~ 2 down to experimental values [8, 17].

In order to illustrate the above mechanism in more detail, we introduce a discretized, exactly soluble, version of the above model, which captures the essential physics. We map the external tangent vector, $\mathbf{t}(s)$, to \mathbf{t}_i ($s = \ell_0 i$) and an internal variable $1 - 2\Theta(\rho(s) - \rho_0 - \lambda)$ (with Θ the step function) to an Ising variable: $\sigma_i = 1$ for an unbroken bond (state A) and $\sigma_i = -1$ for a broken one (B). Each link vector can be denoted by the solid

angle $\Omega_i = (\theta_i, \phi_i)$. The energy $H[\sigma_i, \mathbf{t}_i]$ of a state is

$$H = \sum_{i=1}^{N-1} \tilde{\kappa}_{i,i+1} (1 - \mathbf{t}_i \cdot \mathbf{t}_{i+1}) + H_1(\tilde{J}, \tilde{K}, \tilde{\mu}), \quad (5)$$

$$H_1 = - \sum_{i=1}^{N-1} \left[\tilde{J} \sigma_i \sigma_{i+1} + \frac{\tilde{K}}{2} (\sigma_i + \sigma_{i+1}) \right] - \tilde{\mu} \sum_{i=1}^N \sigma_i.$$

Thus βH contains only the dimensionless parameters $\kappa_{i,i+1} \equiv \beta \tilde{\kappa}_{i,i+1}$, $J \equiv \beta \tilde{J}$, $\mu \equiv \beta \tilde{\mu}$, and $K \equiv \beta \tilde{K}$. This type of model was introduced in the context of helix-coil transitions in 2D [18] and later used in various forms to study DNA force-extension and cyclization [11, 12, 13]. The first term in H , corresponding to H_{ext} in the continuum model, is the bending energy of a discrete WLC with a local rigidity $\kappa_{i,i+1} = \kappa_A = \beta\kappa_b^{ds}/\ell_0$ for a nearest neighbor link of type A-A, $\kappa_B = 2\beta\kappa_b^{ss}/\ell_0$ for B-B and κ_{AB} for A-B. In the Ising part, H_1 , the first term mimics the gradient terms in Eq. (2) and accounts for the local destacking energy [8]. The second term accounts for the difference in stacking energy between a segment of dsDNA and a denaturation bubble. The third term corresponds to the energy ($2\tilde{\mu}$) required to break a base pair, contributing to D in the continuum model. There is evidence that $\tilde{K} \ll \tilde{\mu}$, which justifies the choice of $\tilde{K} = 0$ adopted below [19]. The bare parameters of the internal (Ising) system \tilde{J} , $\tilde{\mu}$, and \tilde{K} are taken to be independent of temperature and bubble loop entropy is not explicitly included; the melting transition is therefore driven only by the difference in bending rigidity. The partition function $Z = \sum_{\{\sigma_i\}} \int \prod_i \frac{d\Omega_i}{4\pi} e^{-\beta H[\sigma_i, \mathbf{t}_i]}$ in transfer kernel form is

$$Z = \sum_{\{\sigma_i = \pm 1\}} \prod_{i=1}^N \int \frac{d\Omega_i}{4\pi} \langle V | \sigma_1 \rangle \langle \sigma_1 | \hat{P}(\Omega_1, \Omega_2) | \sigma_2 \rangle \cdots \cdots \langle \sigma_{N-1} | \hat{P}(\Omega_{N-1}, \Omega_N) | \sigma_N \rangle \langle \sigma_N | V \rangle, \quad (6)$$

where $|V\rangle = (e^{\mu/2}, e^{-\mu/2})$ is the end vector, which enters to account for the free chain boundary conditions, and $\hat{P}(\Omega_i, \Omega_{i+1})$ is the transfer kernel given by

$$\hat{P} = \begin{pmatrix} e^{\kappa_A [\cos \gamma_i - 1] + J + \mu + K} & e^{\kappa_{AB} [\cos \gamma_i - 1] - J} \\ e^{\kappa_{AB} [\cos \gamma_i - 1] - J} & e^{\kappa_B [\cos \gamma_i - 1] + J - \mu - K} \end{pmatrix} \quad (7)$$

with $\cos \gamma_i = \mathbf{t}_i \cdot \mathbf{t}_{i+1}$. The A and B states form the canonical base, $|A\rangle = | + 1 \rangle = (1, 0)$ and $|B\rangle = | - 1 \rangle = (0, 1)$. Thanks to the rotational symmetry of the bending energy we can again integrate out the chain, leading to an effective Ising model with a free energy, $H_{I,0}$, containing renormalized parameters: $Z = e^{-(N-1)\Gamma_0} \sum_{\{\sigma_i\}} e^{-\beta H_{I,0}[\sigma_i]}$ where $H_{I,0} \equiv H_1(\tilde{J}_0, \tilde{K}_0, \tilde{\mu})$ with $J_0 \equiv J - [G_0(\kappa_A) + G_0(\kappa_B) - 2G_0(\kappa_{AB})]/4$ and $K_0 \equiv K - [G_0(\kappa_A) - G_0(\kappa_B)]/2 \equiv K - \Delta G_0^{AB}/2$ the renormalized Ising parameters, and $\Gamma_0 \equiv [G_0(\kappa_A) + G_0(\kappa_B) + 2G_0(\kappa_{AB})]/4$. These parameters depend on chain rigidities through $G_0(\kappa)$ which is the free energy of a single

joint (two monomer) subsystem with rigidity κ : $G_0(\kappa) = -\ln\{\int \frac{d\Omega}{4\pi} \exp[\kappa(\cos(\theta) - 1)]\} = \kappa - \ln[\sinh(\kappa)/\kappa]$. The renormalized quantity $2L_0 \equiv 2(\mu + K_0)$ corresponds to βD_R in the continuum model. If the bending free energy gain in opening one link, ΔG_0^{AB} , is greater than the intrinsic energy cost, $2(\mu + K)$, of opening an interior bond, then L_0 becomes negative, signaling a change in stability of the A and B states. In the limit of high κ_A and κ_B , the entropic contribution dominates: $G_0(\kappa) \approx -S_0(\kappa)/k_B \approx \ln(2\kappa)$. The discrete model then reduces to the continuum one and $\Delta G_0^{AB} \approx \ln(\kappa_A/\kappa_B)$ corresponds to the correction appearing in βD_R . The difference between L_0 and μ when $K_0 \neq 0$ creates an end-interior asymmetry that plays an important role in finite size effects.

The Ising partition and correlation functions are obtained using transfer matrix techniques. The eigenvectors, $|0, \pm\rangle$, and the eigenvalues, $\lambda_{0, \pm} = e^{J_0 - \Gamma_0} [\cosh(L_0) \pm (\sinh^2(L_0) + e^{-4J_0})^{1/2}]$, of the effective Ising transfer matrix allow us to calculate the (dimensionless) free energy per Ising spin of the coupled system, $F = -\ln Z/N$, where $Z = \sum_{\tau=\pm} \langle V|0, \tau\rangle^2 \lambda_{0, \tau}^{N-1}$. The average of the internal state variable is $\langle c \rangle = \langle \sum_{i=1}^N \sigma_i/N \rangle = -\partial F/\partial \mu$, from which the fractions of A and B links, $\varphi_A = (1 + \langle c \rangle)/2$ and $\varphi_B = 1 - \varphi_A$, can be derived. The melting temperature T_m is then defined by $\varphi_B(T_m) = 1/2$. When $N \rightarrow \infty$, $\langle c \rangle$ gets simplified to

$$\langle c \rangle_\infty \equiv \frac{\partial \ln \lambda_{0,+}}{\partial \mu} = \frac{\sinh(L_0)}{[\sinh^2(L_0) + e^{-4J_0}]^{1/2}}. \quad (8)$$

If L_0 vanishes at a temperature, T_m^∞ , sufficiently low for the cooperativity, or loop initiation, factor, $\sigma \equiv e^{-4J_0}$, in the denominator to be small, then the system will undergo a melting transition: $\langle c \rangle_\infty$ will sharply cross-over from +1 for $T < T_m^\infty$ (pure A state) to -1 for $T > T_m^\infty$ (pure B state). *Contrary to previous Ising-type models, the melting temperature is not put in by hand but emerges naturally from $L_0 = 0$.* In Eq. (8) e^{-4J_0} determines the width of the transition region: $\Delta T_m^\infty \equiv 2|\partial \langle c \rangle_\infty / \partial T|_{T_m^\infty}^{-1} \approx (2k_B(T_m^\infty)^2/\tilde{\mu}) \exp[-2J_0(T_m^\infty)]$. In the limit $N, i \rightarrow \infty$, the influence of end-monomers disappears and the Ising correlation function reduces to $\langle (\sigma_i - \langle c \rangle_\infty)(\sigma_{i+r} - \langle c \rangle_\infty) \rangle \rightarrow (1 - \langle c \rangle_\infty^2) \exp(-r/\xi_I)$, where $\xi_I = -\ln^{-1}(\lambda_{0,-}/\lambda_{0,+})$ is the Ising correlation length, the typical size of B (A) domains below (above) T_m .

The tangent-tangent correlation function, $\langle \mathbf{t}_i \cdot \mathbf{t}_{i+r} \rangle$, is obtained using the full transfer kernel method [17], which requires solving a spinor eigenvalue problem: $\hat{P}|\hat{\Psi}\rangle = \lambda|\hat{\Psi}\rangle$, where $|\hat{\Psi}(\Omega)\rangle = (\Psi_{+1}(\Omega), \Psi_{-1}(\Omega))$. We find eigenvalues, $\lambda_{l, \tau}$, labeled by $l = 0, \dots, \infty$ and $\tau = \pm$ with the same form as for $l = 0$ given above, but now where G_0 in the renormalized parameters is replaced by $G_l(\kappa) = \kappa - \ln[\kappa^l(d/\kappa d\kappa)^l(\sinh(\kappa)/\kappa)]$ [20]. The eigenspinors are $|\hat{\Psi}_{l, m; \tau}(\Omega)\rangle = \sqrt{4\pi} Y_{lm}(\Omega) |l, \tau\rangle$ with $Y_{lm}(\Omega)$ the spherical harmonics. The transfer kernel can be expanded in terms of the eigenspinors $\hat{P} = \sum_{l, m, \tau} \lambda_{l, \tau} |\hat{\Psi}_{l, m; \tau}\rangle \langle \hat{\Psi}_{l, m; \tau}|$ and

then be used to calculate the correlation functions. In the limit $N, i \rightarrow \infty$, the expression for the tangent-tangent correlation function simplifies to

$$\langle \mathbf{t}_i \cdot \mathbf{t}_{i+r} \rangle \xrightarrow{N, i \rightarrow \infty} \sum_{\tau=\pm} \langle 1, \tau | 0, + \rangle^2 \exp[-r/\xi_{1, \tau}^p] \quad (9)$$

which reveals the importance of the two persistence lengths, $\xi_{1, \pm}^p = -\ln^{-1}(\lambda_{1, \pm}/\lambda_{0, +})$ (units of ℓ_0). It is not possible to extract from $\langle \mathbf{t}_i \cdot \mathbf{t}_{i+r} \rangle$ one unique length for the whole range of T , because the weights associated with $\xi_{1, \pm}^p$ strongly vary with T .

We now compare the discrete model predictions with experiment [1] by focusing on the melting profile, $\varphi_B(T)$, of a synthetic nonalternating homopolynucleotide, polydA-polydT. A typical profile for a homopolynucleotide has a sigmoidal shape characterized by T_m and ΔT_m . Of the five independent parameters that appear in the theory when $K = 0$, three are determined experimentally (polymerization index N and bending moduli assuming $\kappa_{AB} = \kappa_A$ [17]) and two ($\tilde{\mu}$ and \tilde{J}) are determined by fitting the model to experiment, hence $T_m = T_m(\tilde{\mu}, \tilde{J}; N, \kappa_A, \kappa_B)$. Figure 1a shows $\varphi_B(T)$ for DNA of molecular weight 1180 kDa [1]. From the known persistence lengths we obtain $\kappa_A = 147$ and $\kappa_B = 5.54$ at 300 K. The solid line corresponds to our model fit with $\tilde{\mu} = 4.46$ kJ/mol and $\tilde{J} = 9.13$ kJ/mol, leading to $T_m = 326.4$ K. The fitted value for $2\tilde{\mu}$ is close to the experimental energy of 10.5 kJ/mol needed to break an A-T link [3]. The value for $\tilde{J} \sim 2\tilde{\mu}$ is also consistent with the idea that destacking energy makes the dominant contribution to DNA stability [1]. The renormalized cooperativity parameter at T_m is $\tilde{J}_0 = 11.5$ kJ/mol $> \tilde{J}$. The model fit thus leads to parameter values in accord with experiment (in reality, the fitted values of $\tilde{\mu}$ and \tilde{J} implicitly compensate for effects like loop entropy explicitly left out of the model [1, 17]). In Fig. 1a, the curve corresponding to $N \rightarrow \infty$ is shown for the same parameter values. In this case, $\varphi_B(T)$ is given by Eq. (8) and T_m^∞ is obtained from $L_0 = 0$: $k_B T_m^\infty \simeq 2(\tilde{\mu} + \tilde{K})/\ln(\tilde{\kappa}_A/\tilde{\kappa}_B)$. In this limit the transition width is non-zero, due to the finite cooperativity parameter: $\Delta T_m^\infty \propto \xi_I^{-1}(T_m^\infty) = 2 \exp[-2J_0(T_m^\infty)]$. Since $\xi_I(T_m^\infty) \sim 2000$, typical helix and bubble domains are flexible within a small window about T_m^∞ . When N decreases, the width increases (Fig. 1a) roughly as $\Delta T_m(N) - \Delta T_m^\infty \sim N^{-1}$. Hence even for a long polymer ($N \sim 10^3$), finite size effects are non-negligible, in agreement with experiments [21]. Then the nature of end monomers becomes important, as confirmed in Fig. 1a, which shows how short chains begin to melt by end-unwinding at lower temperatures (the trend that T_m increases with decreasing N will likely be reversed when loop entropy is included [2, 17]). Our model predictions for experimentally accessible A-T pair quantities are in agreement with accepted values [4, 5]: i) $\sigma \approx 10^{-7}$ at T_m ; and at physiological temperature ii) an interior single base-pair opening probability of 10^{-6} with a bub-

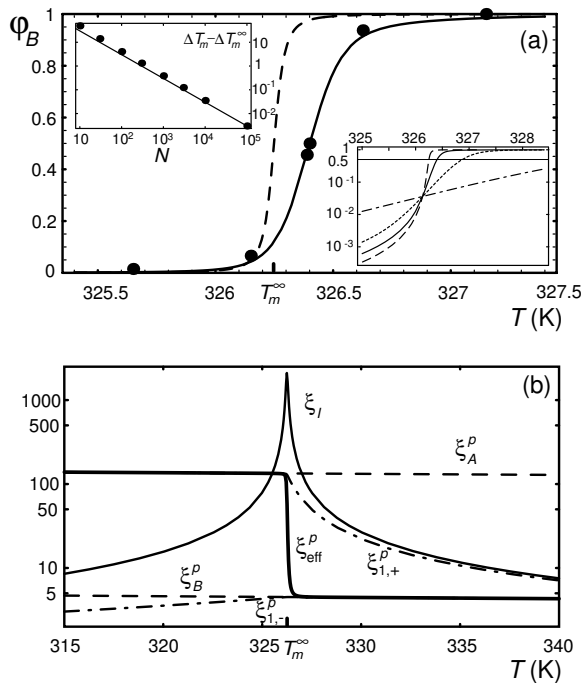


FIG. 1: (a) Melting curves (Fraction of broken base-pairs vs. temperature) for polydA-polydT (data for 0.1 SSC (= 0.015M NaCl +0.0015M sodium citrate, pH 7.0), $N=1815$ [1]). The solid line represents the theoretical result for $\tilde{\mu} = 1.64 k_B T_m$, $\tilde{J} = 3.35 k_B T_m$ ($T_m = 326.4$ K). The broken line corresponds to $N \rightarrow \infty$ (same parameter values). Lower inset: melting curves for $N = 100, 500, 1815, \infty$ (in decreasing order at low temperature, $T < 326$ K); Upper inset: Model results for the shift in transition width $\Delta T_m - \Delta T_m^\infty$ vs. polymer length [24]. (b) Temperature variation ($N \rightarrow \infty$) of the Ising correlation length, ξ_I ; persistence lengths of the coupled system, ξ_{eff}^p and $\xi_{1,\pm}^p$; and of the pure chains, $\xi_{A,B}^p$ (in units of ℓ_0). At T_m^∞ , the effective persistence length, ξ_{eff}^p , rapidly crosses over from ξ_A^p to ξ_B^p .

ble initiation barrier of $17k_B T$, and iii) a free energy of $0.18k_B T$ for breaking an additional base-pair in an already existing bubble.

In contrast to purely Ising-type models, included in the predictions of our theory are mechanical and structural features of the fluctuating chain, such as persistence length or mean-square-radius, $R \equiv \langle \mathbf{R}^2 \rangle^{1/2}$ with $\mathbf{R} = \ell_0 \sum_i \mathbf{t}_i$. From the expression for R in the limit $N \rightarrow \infty$, we can define an effective persistence length, ξ_{eff}^p : $R^2 \simeq (2\ell_0^2 N) \xi_{\text{eff}}^p = (2\ell_0^2 N) \sum_{\tau=\pm} \langle 0, +|1, \tau \rangle^2 \xi_{1,\tau}^p$. Due to the coupling between bending and internal states, the respective weights $\langle 0, +|1, \pm \rangle^2$ associated with each correlation length change abruptly at T_m (cf. Fig. 1b). Since the transition is very abrupt, it should also be possible to observe it experimentally by measuring the radius of gyration by tethered particle motion [22], light scattering, or viscosity experiments. For instance, since the *relative viscosity* is proportional to R^3 , it should clearly exhibit an abrupt thermal transition. Such a transition has indeed been observed for the viscosity of synthetic

homopolynucleotide solutions [23], in qualitative agreement with Fig. 1b. Incorporating bending rigidity into DNA denaturation models thus allows us to make explicit predictions for both melting profiles and DNA mean-size dependent quantities. It will be of great interest to both probe such effects by carrying out experiments on DNA homopolymers and other biopolymers undergoing helix-coil transitions and extend our theory to heteropolymers, mechanical denaturation, and DNA dynamics.

-
- [1] R.M. Wartell and E.W. Montroll, *Adv. Chem. Phys.* **22**, 129 (1972); O. Gotoh, *Adv. Biophys.* **16**, iii (1983).
 - [2] D. Poland and H.R. Scheraga, *Theory of Helix Coil Transition in Biopolymers* (Academic Press, New York, 1970).
 - [3] F. Pincet *et al.*, *Phys. Rev. Lett.* **73**, 2780 (1994).
 - [4] A. Krueger, E. Protozanova and M.D. Frank-Kamenetskii, *Biophys. J.* **90**, 3091 (2006).
 - [5] H.C. Fogedby and R. Metzler, *Phys. Rev. Lett.* **98**, 070601 (2007); A. Bar, Y. Kafri and D. Mukamel, *Phys. Rev. Lett.* **98**, 038103 (2007).
 - [6] Y. Kafri, D. Mukamel and L. Peliti, *Phys. Rev. Lett.* **85**, 4988 (2000).
 - [7] E. Carlon *et al.*, *Phys. Rev. Lett.* **88**, 198101 (2002).
 - [8] M. Peyrard and A.R. Bishop., *Phys. Rev. Lett.* **62**, 2755 (1989); T. Dauxois, M. Peyrard, and A.R. Bishop., *Phys. Rev. E* **47**, 684 (1993).
 - [9] J.-H. Jeon, W. Sung and F.H. Ree, *J. Chem. Phys.* **124**, 164905 (2006).
 - [10] Y. Gao, K.V. Devi-Prasad and E.W. Prohovsky, *J. Chem. Phys.* **80**, 6291 (1984).
 - [11] J. Yan and J.F. Marko, *Phys. Rev. Lett.* **93**, 108108 (2004).
 - [12] C. Storm and P.C. Nelson, *Europhys. Lett.* **62**, 760 (2003).
 - [13] P. Ranjith, P.B. Sunil Kumar and G.I. Menon, *Phys. Rev. Lett.* **94**, 138102 (2005).
 - [14] N. Korolev, A.P. Lyubartsev and L. Nordenskiöld, *Biophys. J.* **75**, 3041 (1998).
 - [15] R.M. Fye and C.J. Benham, *Phys. Rev. E* **59**, 3408 (1999).
 - [16] In reality, κ_s in Eq. (2) should include an enthalpic shear modulus term accounting for DNA stacking energy [8].
 - [17] J. Palmeri, M. Manghi and N. Destainville, in preparation (2007).
 - [18] J. Palmeri and S. Leibler, *Dynamical Phenomena at Interfaces, Surfaces and Membranes* (Eds. D. Beysens *et al.*, Nova Science Publishers, Inc., New York, 1993).
 - [19] D.P. Aalberts, J.M. Parman and N.L. Goddard, *Biophys. J.* **84**, 3212 (2003).
 - [20] G.S. Joyce, *Phys. Rev.* **155**, 478 (1967).
 - [21] G. Altan-Bonnet, A. Libchaber and O. Krichevsky, *Phys. Rev. Lett.* **90**, 138101 (2003).
 - [22] N. Pouget *et al.*, *Nucleic Acids Res.* **32**, e73 (2004).
 - [23] R.B. Inman and R.L. Baldwin, *J. Mol. Biol.* **8**, 452 (1964).
 - [24] All curves cross at $T \simeq 326.1$ K, where effects due to the difference in renormalized stacking energy ($\sim K_0$) exactly compensate those due to renormalized destacking ($\sim J_0$) [17].